Scripta Materialia 108 (2015) 40–43

Contents lists available at ScienceDirect

Scripta Materialia

journal homepage: www.elsevier.com/locate/scriptamat

Increased viewing angle and light extraction efficiency of flip-chip light-emitting diode using double-side patterned sapphire substrate

Kuan-Chieh Huang [a,*], Yi-Ru Huang [b], Chun-Ming Tseng [a], Snow H. Tseng [b], Jing-En Huang [a]

[a] R&D Center, Genesis Photonics Inc., Tainan 74144, Taiwan
[b] Graduate Institute of Photonics and Optoelectronics, National Taiwan University, Taipei 10617, Taiwan

ARTICLE INFO

Article history:
Received 18 March 2015
Revised 6 May 2015
Accepted 19 May 2015
Available online 15 June 2015

Keywords:
Flip-chip light-emitting diode
Microstructure
Optical properties
Monte Carlo simulation
Semiconductor

ABSTRACT

Highly optical performances of flip-chip light-emitting diodes, employing double-side patterned sapphire substrates with various heights (0, 280, and 650 nm) of textures on the bottom surfaces of the substrates, are evaluated. At 700 mA, the chip (280 nm) delivers higher power of 728.3 mW in comparison to the characteristics in the cases of 0 nm (708.4 mW) and 650 nm (702.2 mW). A wide radiation pattern as well as a large viewing angle of such a chip is demonstrated.

In a GaN-based flip-chip light-emitting diode (FC-LED), the patterned sapphire substrate (PSS) is indispensable for contributing to the power enhancement of chip [1,2] owing to the predominant effects brought by PSS as follows. One is the reduction of dislocation density of the GaN epitaxial layer, growing on PSS, in favor of the improved internal quantum efficiency. The other is the patterned structure of PSS against the total internal reflection (TIR) at the interface between sapphire and GaN epitaxial layer for benefiting light extraction [3,4]. Over the past few years, much effort has been made aiming to further have more photons escape from the FC-LED by texturing the surface which is opposite to the GaN/sapphire interface of the PSS [5–7]. In addition, several researchers have evaluated the optical performances of FC-LEDs with textures merely forming on the bottom surfaces of PSSs [8,9]. That is, the textured surface of PSS, possessing a mesh-type shape, was designed to achieve the relevant FC-LED with high light extraction efficiency [8]. Furthermore, the FC-LED, applying a PSS with submicron-scale configuration, can facilitate the production of light [9].

Therefore, in this work, we developed a high-power FC-LED based on double-side PSS; three different heights (0, 280, and 650 nm) of patterned structures were created on the bottom surfaces of PSSs facing the surrounding for comparison. The viewing angles and output power of such FC-LEDs were also discussed. Moreover, the simulations regarding the directions of light traveling in the corresponding PSSs were accomplished with the assistance of Monte Carlo ray tracing.

The InGaN/GaN multiple quantum-well (MQW) LEDs were grown on the *c*-plane (0001)-oriented PSSs by using a metal-organic chemical vapor deposition apparatus to acquire a typical LED chip with single-side PSS. The periodic arrays, having a depth of 1.5 μm of the PSS, were prepared by inductively coupled plasma (ICP) etcher. Trimethylgallium, trimethylindium, ammonia, bicyclopentadienyl magnesium, and silane served as the precursors for obtaining Ga, In, N, Mg, and Si, respectively. The growth of epitaxial structure of the LED was carried out according to the previous literature [10]. In brief, the textured surface of PSS was the site at which a GaN nucleation layer grew at the beginning. Afterward, a thick n-type GaN layer (4 μm) doped with Si, a ten-period of InGaN/GaN heterostructure as MQWs, and a p-type GaN layer (120 nm) doped with Mg were vertically arranged on the nucleation layer in sequence.

For the FC-LED process, a transparent conductive layer, indium tin oxide, was included [11]. The p-type and n-type GaN were the layers on which Ti/Au and Ti/Al/Ti/Au metal contacts deposited, respectively, by means of electron beam evaporation [10]. A reflective mirror of Ag was further deposited on the p-contact [12]. Then a defined film based on Au was deposited on the p- and n-contacts [2] to obtain a final single-side PSS-assembled FC-LED chip (designated as LED I hereafter) with a dimension of 1 mm × 1 mm. The optical properties of FC-LEDs reported were characterized using

* Corresponding author.
E-mail addresses: kc_huang@gpiled.com, kchuang0801@gmail.com (K.-C. Huang).

http://dx.doi.org/10.1016/j.scriptamat.2015.05.040
1359-6462/

an integrating sphere, equipped with a Keithley source meter, and a viewing angle instrument.

To convert the foregoing LED I into an FC-LED with double-side PSS, a film of photoresist was coated onto the bottom surface of the LED I followed by photolithography processes (Fig. 1a). The ICP etching was further used to establish a regular array, consisting of patterned structures, on the bottom surface of the LED I, thereby completing the fabrication of the double-side PSS-based FC-LED chip (Fig. 1a). In Fig. 1b, the textures can be clearly observed not only on the outer surface of sapphire, exposed to air, but also at the interface between sapphire and GaN in the as-prepared chip. This confirms the successful formation of the FC-LED with double-side PSS. Thus two different types of pertinent FC-LEDs, including the chip with smaller textures (designated as LED II hereafter) and that owning relatively larger ones (designated as LED III hereafter), were further prepared by adjusting the etching time of ICP. Compared to the small surface roughness of LED I, originating from the bare sapphire substrate (Fig. 2a), both LED II and LED III textures exhibit nearly cone-like morphologies due to the ICP treatments (Fig. 2b and c). In Fig. 2d, the heights of the textures were estimated to be about 280 and 650 nm for LED II and LED III, respectively.

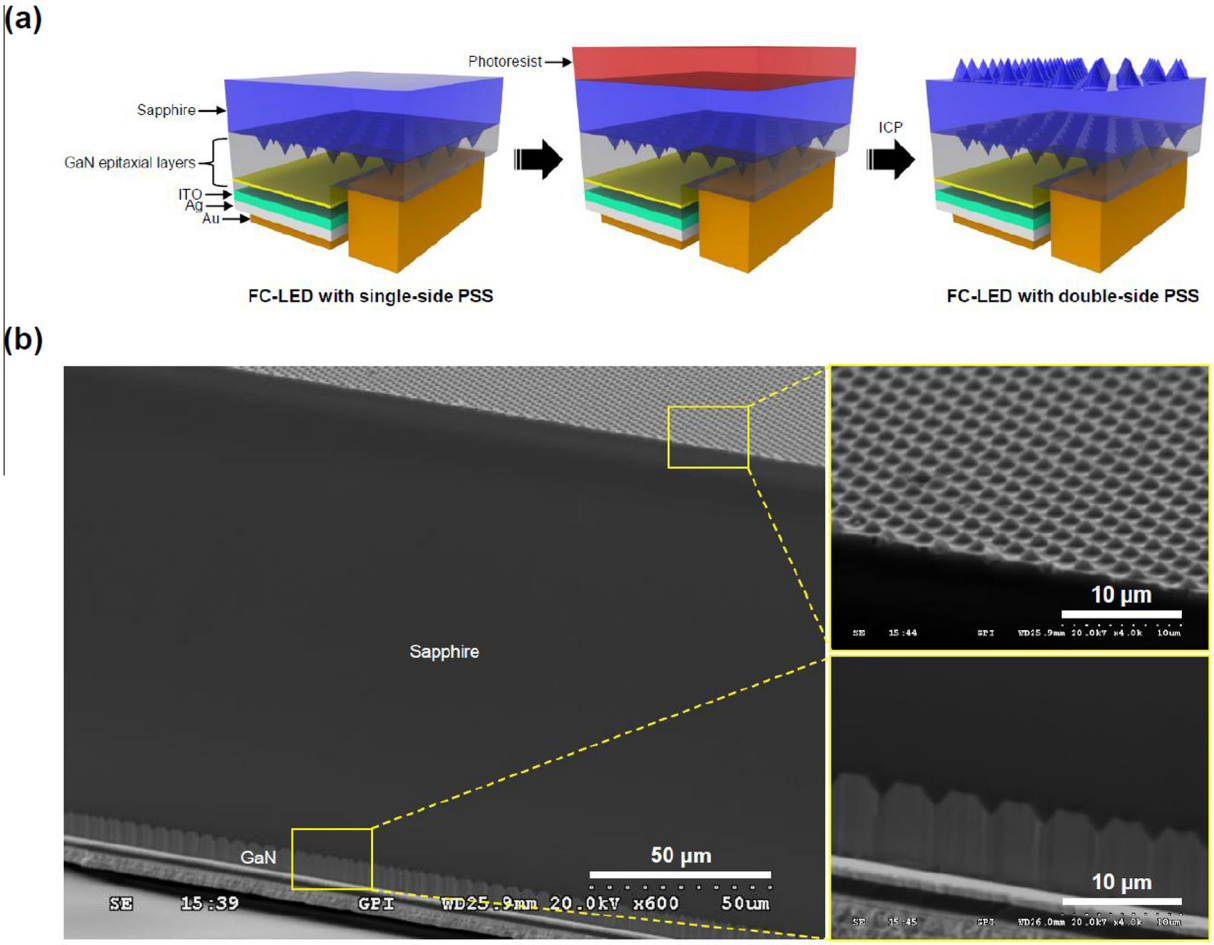

Fig. 1. (a) Schematic process of FC-LED chip with double-side PSS and (b) cross-sectional scanning electron microscope images of the relevant chip, obtained at a tilted angle of sample holder.

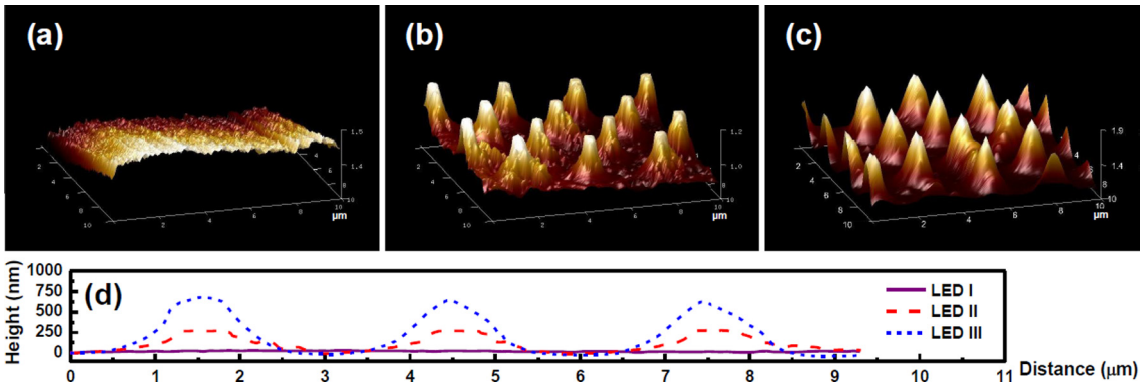

Fig. 2. 3-Dimensional atomic force microscope images of bottom surfaces of sapphire substrates of (a) LED I, (b) LED II, and (c) LED III; (d) their corresponding profiles.

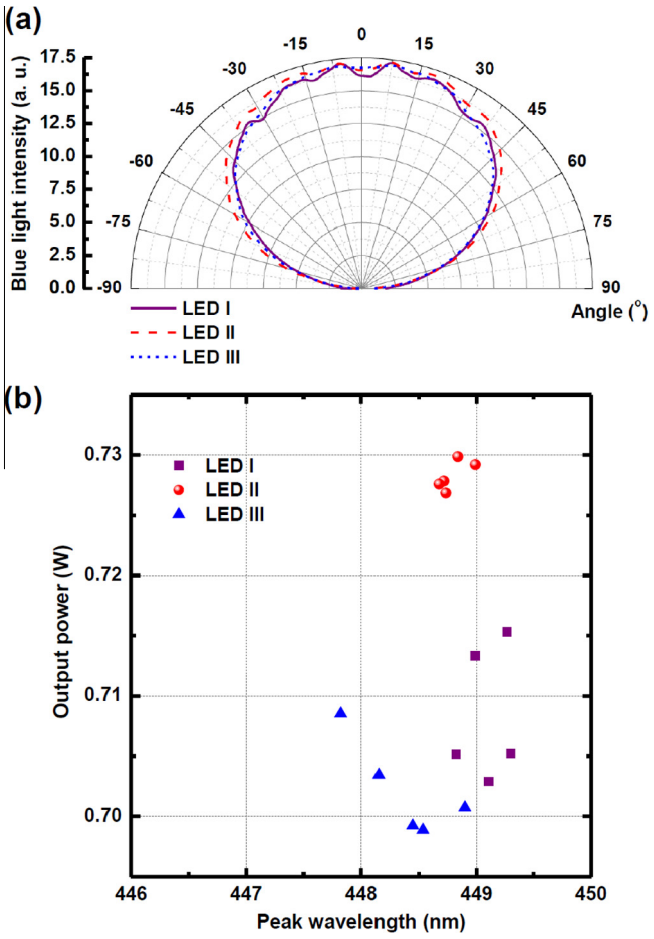

Fig. 3. (a) Far-field radiation patterns and (b) output power *vs.* peak wavelength of LED I, LED II, and LED III.

Under 350 mA injection, the far-field emission patterns of LED I, LED II, and LED III are shown in Fig. 3a. At the full width at half maximum, the LED I delivered a viewing angle of about 131°. However, the viewing angle increased to *ca.* 135° which can be simply observed from the variation in radiation pattern for LED II (Fig. 3a). The wide pattern as well as the large viewing angle of the LED II is explained by the suppression of the TIR at the air/sapphire interface due to the presence of patterned structures on the bottom surface of the chip. When the height of texture of chip increased from 280 nm (LED II) to 650 nm (LED III), the radiation pattern of LED III became narrower than that of LED II (Fig. 3a). This finding implies that a large number of photons, emitted from the MQWs, are reflected by the large textures and return to the LED III, thereby leading to the chance of reabsorption [13]. The effects of height of texture on the ray tracing will be discussed for the LED I, LED II, and LED III at a later stage. Fig. 3b shows the output power in relation to the peak wavelengths of all FC-LEDs with input current of 700 mA. Five independent samples were prepared and analyzed for each type of chip. Although there is a vibration on the wavelength for the obtained data, we believed that this causes only less disturbance to power competition due to most of the data centered in a small range of 448.5 and 449.5 nm (Fig. 3b). The LED II gave the best performance of an average value of 728.3 mW among three cases of LED I (708.4 mW), LED II, and LED III (702.2 mW). The enhanced power, generated from the LED II, is attributed to a large portion of light emerging via the patterned structures, with reference to the power given by LED I. The result is consistent with the difference in radiation patterns between the cases of LED I and LED II (see Fig. 3a). On the other hand, a better light output of the LED II, compared to that of the LED III, can be explained by the subsequent results of Monte Carlo ray tracing obtained through TracePro software [14].

In Fig. 4, we made simulation analyses to determine the impact of textures with 0, 280, and 650 nm in heights in accordance with the cross-sections of patterned geometries of PSSs on the bottom surfaces of LED I, LED II, and LED III (see Fig. 2d) on the optical ray tracing from sapphire to air. The refractive indices of air and sapphire were set to be 1 and 1.78, respectively. To simplify the investigation, one single texture was merely chosen for the study in each case. Also we focused on the ray tracing behavior depending on the directions of light, following the arrows (Fig. 4). In Fig. 4a, the paths of LED I, LED II, and LED III were initially simulated corresponding to the θ_1 of 45° [$\theta_1 = \tan^{-1}(10/10)$], which

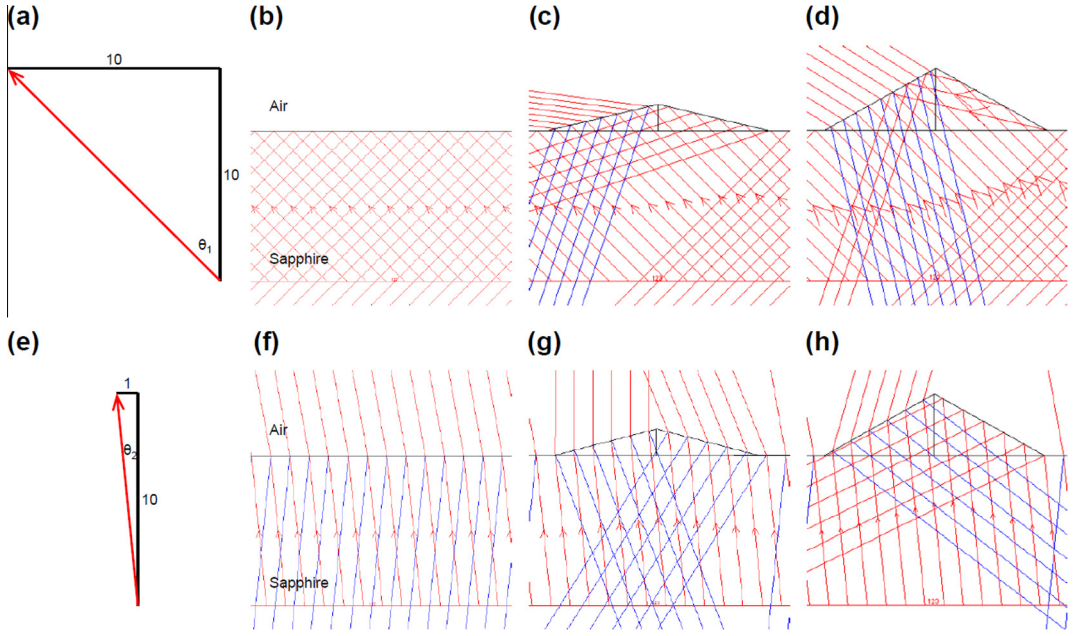

Fig. 4. (a) Simulation using θ_1 and relevant ray tracing of (b) LED I, (c) LED II, and (d) LED III. (e) Simulation using θ_2 and relevant ray tracing of (f) LED I, (g) LED II, and (h) LED III.

was larger than the critical angle (θ_c) of 34.2° [$\theta_c = \sin^{-1}(1/1.78)$] at the air/sapphire interface. The rays were thus totally trapped by sapphire for LED I in this situation owing to the TIR (Fig. 4b). However, in Fig. 4c and d, both kinds of the patterned sapphires of LED II and LED III allowed the rays to pass through, thereby making the rays reach the air side. This results from the decreased incident angle at the air/sapphire interface of the texture (LED II or LED III) on the basis of the same θ_1 (45°), with reference to the case of LED I.

On the other hand, a relatively smaller θ_2 of 5.7° [$\theta_2 = \tan^{-1}(1/10)$], compared to θ_1, was discussed (Fig. 4e). In Fig. 4f, the simulated rays using θ_2 can completely escape from the sapphire for LED I because of the corresponding incident angle (5.7°) which is smaller than the critical value (34.2°) at the interface. In the meantime the incident angles at the interface, originating from the LED II with θ_2, still remained at an acceptable level of being light escape cones due to the texture having a favorable height, thus efficiently leading to the rays emerging from both left-hand and right-hand sides of the geometry (Fig. 4g). However, the escape of light was inhibited at the right-hand interface of the LED III by TIR, as shown in Fig. 4h. We reasoned that such a configuration with 650 nm in height has more chances to let the incident angle exceed the tolerance of critical value at the air/sapphire interface, with reference to the case of LED II (280 nm). Overall, when the θ of ray ranges from 5.7° to 45°, the LED II is supposed to produce the most light among the three cases (LED I, LED II, and LED III). The simulation results are consequently consistent with the difference in output power of the FC-LEDs (see Fig. 3b).

In conclusion, the regular and periodic arrays of patterned structures, established on the surface where light escapes, namely the bottom surface of a PSS, in an FC-LED, are promising for contribution to the achievement of relevant chip with high light extraction efficiency under current injection. Most importantly, such a structure, having a well-designed geometry of hump-like shape with adequate height, guarantees the power improvement of the chip. Thus a double-side PSS-assembled FC-LED with textures of 280 nm in height (LED II) gives about 2.8% and 3.7% enhancements in output power in comparison to the performances of the chip with flat bottom surface (LED I) and the chip with textures of 650 nm in height (LED III), respectively. In addition, the viewing angle of the chip with double-side PSS (LED II) is increased by *ca.* 3.1%, with reference to the viewing angle of the chip based on single-side PSS (LED I).

References

[1] S. Nakamura, T. Mukai, M. Senoh, Appl. Phys. Lett. 64 (1994) 1687–1689.
[2] W.K. Wang, D.S. Wuu, S.H. Lin, S.Y. Huang, P. Han, R.H. Horng, Jpn. J. Appl. Phys. 45 (2006) 3430–3432.
[3] Y.C. Lee, C.H. Ni, C.Y. Chen, Opt. Express 18 (2010) A489–A498.
[4] D.S. Wuu, W.K. Wang, K.S. Wen, S.C. Huang, S.H. Lin, R.H. Horng, Y.S. Yu, M.H. Pan, J. Electrochem. Soc. 153 (2006) G765–G770.
[5] J.H. Lee, S.M. Hwang, N.S. Kim, J.H. Lee, IEEE Electron Device Lett. 31 (2010) 698–700.
[6] B.S. Cheng, C.E. Lee, H.C. Kuo, T.C. Lu, S.C. Wang, Jpn. J. Appl. Phys. 48 (2009) 04C115.
[7] C.F. Shen, S.J. Chang, W.S. Chen, T.K. Ko, C.T. Kuo, S.C. Shei, IEEE Photon. Technol. Lett. 19 (2007) 780–782.
[8] D.S. Han, J.Y. Kim, S.I. Na, S.H. Kim, K.D. Lee, B. Kim, S.J. Park, IEEE Photon. Technol. Lett. 18 (2006) 1406–1408.
[9] B.J. Kim, M.A. Mastro, H. Jung, H.Y. Kim, S.H. Kim, R.T. Holm, J. Hite, C.R. Eddy Jr., J. Bang, J. Kim, Thin Solid Films 516 (2008) 7744–7747.
[10] Y.L. Li, Y.R. Huang, Y.H. Lai, IEEE J. Sel. Top. Quantum Electron. 15 (2009) 1128–1131.
[11] Y.C. Lin, S.J. Chang, Y.K. Su, T.Y. Tsai, C.S. Chang, S.C. Shei, C.W. Kuo, S.C. Chen, Solid State Electron. 47 (2003) 849–853.
[12] J.S. Sung, J. Han, D.Y. Noh, T.Y. Seong, Scr. Mater. 80 (2014) 5–8.
[13] K.J. Chen, H.V. Han, B.C. Lin, H.C. Chen, M.H. Shih, S.H. Chien, K.Y. Wang, H.H. Tsai, P. Yu, P.T. Lee, C.C. Lin, H.C. Kuo, IEEE Electron Device Lett. 34 (2013) 1280–1282.
[14] K.Y. Liao, S.H. Tseng, Solid State Electron. 104 (2015) 96–100.